Analytica Chimica Acta 1225 (2022) 340199

Contents lists available at ScienceDirect

Analytica Chimica Acta

journal homepage: www.elsevier.com/locate/aca

In vitro/in vivo degradation analysis of trastuzumab by combining specific capture on HER2 mimotope peptide modified material and LC-QTOF-MS

Li Lu [a,b,1], Xiao Liu [a,1], Chengyi Zuo [a], Jingwei Zhou [a], Chendi Zhu [a], Zhang Zhang [c], Marianne Fillet [a,b], Jacques Crommen [a,b], Zhengjin Jiang [a,c,*], Qiqin Wang [a,c,**]

[a] Institute of Pharmaceutical Analysis, College of Pharmacy, Jinan University, Guangzhou, 510632, China
[b] Laboratory for the Analysis of Medicines (LAM), Department of Pharmacy, CIRM, University of Liege, Avenue Hippocrate 15, B36 Tour 4 +3, 4000, Liège, Belgium
[c] Department of Pharmacy and Guangdong Province Key Laboratory of Pharmacodynamic Constituents of Traditional Chinese Medicine & New Drug Research, Jinan University, Guangzhou, 510632, China

HIGHLIGHTS

- A bioanalytical platform was developed using mimotope peptide modified material and LC-QTOF-MS.
- HER2 mimotope peptide can precisely recognize trastuzumab from serum samples.
- Dynamic monitoring of modifications of trastuzumab was realized using the platform.
- Deamidation, isomerization, oxidation or cyclization of key sites were verified.
- This platform exhibited superior specificity than Protein A based methods.

GRAPHICAL ABSTRACT

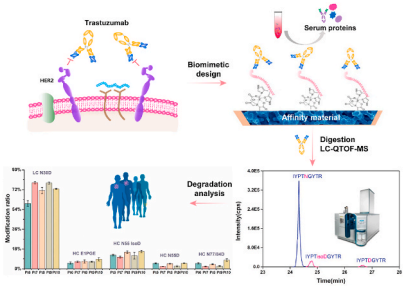

ARTICLE INFO

Keywords:
Therapeutic monoclonal antibody
Affinity enrichment
Degradation study
LC-QTOF-MS
Breast cancer patient serum

ABSTRACT

Degradation analysis of therapeutic mAb is of high interest for critical quality attributes assessment and biotransformation studies. However, some obstacles, including low in vivo concentrations of mAb and complex biological matrices containing IgGs, could seriously interfere with mAb bioanalysis. In this study, a bioanalytical platform was developed for studying in vitro/in vivo modifications of trastuzumab, in which specific capture on mimotope peptide modified material was combined with trypsin digestion and LC-QTOF-MS analysis. It is worth noting that this material exhibits high specificity, suitable dynamic binding capacity, very little non-specific protein adsorption, and thus provides good enrichment and quantification performances for trastuzumab from patient serums. In particular, this bioanalytical platform was successfully applied to the dynamic monitoring of modifications of trastuzumab, such as deamidation, isomerization, oxidation and cyclization. Except for the faster deamidation of LC-Asn-30 and HC-Asn-387/392/393 under serum incubation, similar degradation trends for other sites were observed in phosphate buffer and spiked serum. Differences of peptide modification degrees of trastuzumab in patient serums were also observed. The novel platform exhibited superior specificity than Protein A/G/L based analytical methods, lower cost and higher stability than antigen or anti-idiotypic antibody based analytical methods, ensuring the evaluation of modification sites.

* Corresponding author. Institute of Pharmaceutical Analysis, College of Pharmacy, Jinan University, Guangzhou 510632, China.
** Corresponding author. Institute of Pharmaceutical Analysis, College of Pharmacy, Jinan University, Guangzhou 510632, China.
E-mail addresses: jzjjackson@hotmail.com (Z. Jiang), qiqinxtu@163.com (Q. Wang).
[1] These authors contributed equally to this work.

https://doi.org/10.1016/j.aca.2022.340199
Received 18 May 2022; Received in revised form 12 July 2022; Accepted 22 July 2022
Available online 31 July 2022

1. Introduction

Therapeutic monoclonal antibodies (mAbs) are now one of the most successful and important treatment for patients with hematological malignancies and solid tumors [1–4]. Recently, the biotransformation study of therapeutic mAbs after in vivo administration has gained great attention due to the fact that some modifications could decrease the biological activity, impact the pharmacokinetics, or increase immunogenicity of the target drug [5,6]. For instance, it has been demonstrated in several studies that asparagine (Asn) deamidation and aspartic acid (Asp) isomerization to iso-aspartic acid cause decreased antigen-binding affinity, including modifications in heavy chain complementarity determining regions 1 and 2 (CDR1 and CDR2), and light chain CDR1 and CDR3 [7–10]. Unlike deamidation and isomerization, methionine (Met) oxidation usually happened at the interface of the C_H2 and C_H3 domains of the constant region, which has been reported to decrease the FcRn binding affinity and circulation half-life of mAbs [10], but could also happen in the CDRs and impact antigen-binding affinity [11]. In addition, pyroglutamate (pGlu) formation may also influence target binding due to the fact that the N-termini of both the heavy and light chains of mAbs are in the variable region near the CDR [12]. Therefore, the monitoring of in vivo mAb degradation is crucial for the efficacy and risk assessment in early drug development, and the understanding of the metabolism and elimination of mAbs in clinical studies.

However, in vivo degradation study of mAbs is not widely performed because of the limited sample supply, low drug concentrations, complex biological matrices containing high levels of endogenous IgGs (7–18 mg/mL) [13], and in particular the use of traditional ligand-binding assays without structural characterization ability [14]. To meet these challenges, hybrid immunoaffinity LC-MS platforms based on antigens or anti-idiotypic antibodies were recently established to assess the key amino acid modifications of mAbs in humans [13–17]. Although hybrid immunoaffinity LC-MS offers unparalleled specificity and unambiguous identification, the drawbacks of antigen or anti-idiotypic antibody-based affinity materials cannot be neglected, including long discovery time of affinity ligands, high manufacturing and processing costs, ligand instability, and risk of ligand leakage from support matrices [18–20]. Moreover, traditional support materials (sepharose and agarose) present certain disadvantages, such as gel compressibility, poor pore diffusion, mass transfer limitations, and some non-specific adsorption [21,22]. Therefore, a novel platform based on an affinity material with excellent specificity and stability is requested.

Thanks to their wide diversity, better chemical stability, moderate affinity for the target protein, lower cost and immunogenicity than biomacromolecules [23–26], small peptides showed fascinating prospects for a broad range of applications, such as medicines [27], biomaterials [28], biosensors [29], and separation science [30–32]. In particular, mimotope peptides can mimic an epitope of a specific antigen and thus bind to the antigen-binding (Fab) region or paratope of the corresponding antibody [33,34]. To date, few mimotope peptide-based affinity membranes were reported to specifically capture the target mAb from biological fluids containing IgGs [35,36]. However, except for the inherent drawbacks (poor mechanical strength and easy clogging) of membrane, non-specific serum protein adsorption [35], too strong affinity (nM level) of ligand, requirement of denaturating elution conditions (2% sodium dodecyl sulfate, 100 mM dithiothreitol) [35,36] were also observed on these mimotope peptide-based affinity membranes, which will result in antibody inactivation and incompatibility with downstream LC-QTOF-MS analysis [37]. Cumbersome method for the sodium dodecyl sulfate (SDS) removal such as dialysis often result in significant loss of the target protein [37], therefore affect their application to in vivo degradation analysis of the target mAb.

Some studies reported that a histidine tag may induce particular folding patterns of the peptide in the presence of metal ions [38] or interfere the interaction between protein and ligand [39], which would regulate the affinity behavior of the peptide ligand towards the target protein. Moreover, porous polymeric materials can overcome the drawbacks of sepharose, agarose, and membrane because of their high mechanical strength and permeability, good biocompatibility, and negligible non-specific protein adsorption [40]. Therefore, to mimic the affinity interactions between human epidermal growth factor receptor 2 (HER2) and trastuzumab, a mimotope peptide (HHHH HHGSGSGSQLGPYELWELSH, HH24) functionalized polymeric material was developed in this study. The rationally designed peptide ligand HH24 exhibited affinity to trastuzumab at μM level and thus could overcome the shortcoming of denaturating elution conditions needed for traditional enrichment materials. In particular, a novel bioanalytical platform was proposed for in vitro/in vivo degradation analysis of trastuzumab in biological fluids by combining HH24 modified polymeric material, trypsin digestion, and LC-QTOF-MS. After optimization of the operating conditions, the feasibility of the platform was assessed by monitoring the in vitro degradation of trastuzumab in time-course studies. The peptide modification trends and sites for trastuzumab in pH 7.4 phosphate buffer (PB) and spiked human serum were compared. Finally, in vivo modification analyses of trastuzumab in HER2 positive breast cancer patients treated with this mAb were carried out using the platform to verify its practical application potential.

2. Experimental section

2.1. Evaluation of specific interactions between HH24 peptide and trastuzumab by microscale thermophoresis (MST) and computational analysis

Firstly, trastuzumab was labeled using the Protein Labeling Kit Monolith™ RED-NHS (MO-L011, Nano Temper, Beijing, China). According to the manufacturer's protocol, the labeling reaction was performed by employing a concentration of 10 μM trastuzumab (molar ratio dye: protein = 1:1) at room temperature for 30 min. The supplied dye removal column used to eliminate the unreacted dye was equilibrated with 1 mL MST buffer (20 mM PB, 0.05% Tween-20). The degree of labeling was evaluated by UV spectrophotometry at 650 and 280 nm.

The labeled trastuzumab concentration was then adjusted to 320 nM with MST buffer. The HH24 peptide was dissolved in MST buffer and a series of 1:1 dilutions were prepared using the same buffer, resulting in concentrations ranging from 0.152 to 5040 μM for HH24. For the measurements, 10 μL of each peptide solution were mixed with 10 μL labeled trastuzumab, which led to a final concentration of trastuzumab of 160 nM. After 10 min incubation, the mixed sample was transferred into standard Monolith NT.115 Capillaries for MST. MST measurements were performed using a Monolith NT.115 instrument (Nano Temper, Beijing, China) at a temperature of 25 °C. Instrument parameters were adjusted to 20% LED power and medium MST power.

Molecular docking and molecular dynamics simulation analyses (details are shown in Supporting Information S1.3) were further used to evaluate the specific interactions between HH24 peptide and trastuzumab.

2.2. Fabrication and evaluation of the HH24 modified affinity material

The preparation of Ni^{2+} based immobilized metal-affinity chromatography (IMAC) material was performed in pipettes according to a previously described method [32]. HH24 peptide was then immobilized on the material surface via a metal ion chelation reaction between the histidine tag of the peptide (0.5 mg/mL, 200 μL) and Ni^{2+}. The affinity material was also prepared in capillaries, rinsed with methanol to remove unreacted reagents and fully dried. Capillaries were cut into 3 mm sections for scanning electron microscopy (SEM) and energy-dispersive spectroscopy (EDS) analysis. The material in the pipettes was used for thermogravimetric analysis (TGA), Fourier transform infrared spectroscopy (FT-IR), water contact angle, and pore size distribution analysis.

The target recognition ability of the affinity material was verified by testing protein mixture (including trastuzumab, HSA, lactoferrin, thrombin, or hIgG). The affinity material was first equilibrated with 1 mL, 20 mM phosphate buffer containing 150 mM NaCl, 0.05% Tween-20, pH 7.4 (buffer A). Then, 100 μL protein mixture were loaded and the unretained proteins were washed with 500 μL buffer A. The retained proteins were eluted using 400 μL buffer B (10 mM HCOONa, 100 mM NaCl, pH 3.1). All fractions were collected for SDS-PAGE and purity analysis. Purity was calculated based on the SDS-PAGE images using the Image J software.

2.3. Incubation of trastuzumab in PB and human serum

To simulate antibody degradation trends in vivo, trastuzumab was spiked to a final concentration of 0.5 mg/mL in PB (pH 7.4, 20 mM PB) and 0.2/0.5 mg/mL in human serum at 37 °C. The solutions were incubated and sampled over time (0, 4, 7, 14, and 21 days). 0.1% sodium azide was added to prevent bacterial growth. Following incubation, the samples were stored at −80 °C before enrichment and analysis.

2.4. Enrichment of trastuzumab in complex biological samples

The HH24 peptide modified affinity material was employed for the enrichment of trastuzumab from spiked PB, spiked human serum, or patient serum samples. For example, patient serum samples were diluted 3 times with loading buffer (20 mM PB, pH7.4, 150 mM NaCl) and then the diluted samples (200 μL) were loaded onto a pipette containing the affinity material. After equilibration with loading buffer (four column volumes), 10 mL of the buffer A were pumped through the pipette at a flow rate of 8 mL/h to remove the unretained compounds. The remaining proteins were eluted with 400 μL buffer B. All solutions were collected for the peptide mapping analysis. Before digestion, the eluates containing the enriched trastuzumab were desalted using a 10 kDa MWCO filter (Amicon, 0.5 mL, cellulose, Millipore Sigma) and buffer exchange was performed using 10 M urea (pH 8, 100 mM Tris-HCl).

2.5. Peptide mapping analysis

The extent of degradation or biotransformation of the target mAb was estimated by peptide mapping analysis. The enriched trastuzumab was firstly denatured using 10 M urea (pH 8.0, 100 mM Tris-HCl), and the disulfide bonds were reduced with 10 mM dithiothreitol (DTT) at 50 °C for 30 min. To prevent reformation of the disulfide bonds, the free sulfhydryl groups on the cysteine residues were alkylated using 20 mM iodoacetamide (30 min, at room temperature, kept from light) to yield S-acetyl cysteine. Then the buffer of the samples was changed to 100 mM tris-HCl (pH 8.0) by ultrafiltration for digestion with trypsin (protein: trypsin ratio: 25: 1, 3 h) and the digestion was terminated by addition of 0.5% formic acid (FA). The digests were analyzed using an AB Sciex ExionLC system connected to a SCIEX X500R QTOF mass spectrometer, using an Acquity BEH C18 column (Waters, ACQUITY UPLC®BEH C18 1.7 μm, 2.1 × 150 mm) at 60 °C with 0.1% FA in water as mobile phase A and 0.1% FA in acetonitrile as mobile phase B. The gradient started with a 2-min hold at 2% B, followed by an increase to 40% B over 100 min and then an increase to 90% B for 10 min, at a flow rate of 0.2 mL/min. MS and MS/MS analyses were performed in the positive ESI mode with a high-resolution full scan, followed by tandem MS scans of the fifteen most abundant precursor ions. BioPharma view and SCIEX OS software were employed for qualitative and semiquantitative analysis. Modified peptides (by oxidation, deamidation, etc.) were quantitated using integrated peak areas from the extracted ion chromatograms, and results were presented as percentages of total peptide (unmodified and modified) peak areas.

2.6. Patient serum analysis

Ten blood samples were collected from trastuzumab-treated patients with HER2-positive breast cancer (The First Affiliated Hospital of Jinan University). Samples were collected under appropriate ethical approval and after written informed consent of patients. Patient serum samples were prepared immediately after blood collection and stored at −80 °C. The trastuzumab biotransformation analyses in five patient serum samples were performed using the described LC-QTOF-MS method after specific capture on the HH24 peptide modified affinity material.

3. Results and discussion

3.1. Evaluation of HER2 mimotope peptide binding behavior

Firstly, the affinity of HH24 peptide for trastuzumab was evaluated by MST. For comparison, the HER2 mimotope peptides QLGPYELWELSH (QH12) and GSGSGSQLGPYELWELSH (GH18) were also synthesized and investigated. As shown in Fig. 1a and Fig. S1, according to the binding curves, the affinity (K_d value) of QH12, GH18, and HH24 for trastuzumab were 11.2 ± 9.7 μM, 12.7 ± 8.4 μM, and 26.4 ± 16.1 μM, respectively, which are within the normal range (10^{-5}-10^{-7} M) for an affinity peptide towards a protein [23]. These results indicate that the HH24 peptide could recognize trastuzumab with moderate binding strength. A computational analysis was subsequently carried out to identify the potential HH24-trastuzumab interaction sites and the specific residues involved in the binding (Fig. S2). The binding mode of the HH24-trastuzumab complex is illustrated in Fig. 1b. The benzene ring of residue Tyr17 can form π-π conjugated interactions with Tyr33, Tyr105, and Trp99 in the heavy chain. The carboxylic acid group of Glu18 can form a salt bridge with the positively charged residues Arg50 and Arg59 in the heavy chain. Glu21 can form hydrogen bonding interactions with Thr93 and Thr94 in the light chain. The total binding free energy for the HH24 peptide was calculated and a value of −56.12 kcal/mol was found (Table S1), which further confirms that this peptide has good binding affinity to trastuzumab. In particular, the absolute value of electrostatic energy (EEL) is much higher than the van der Waals contribution (VDWAALS), which indicates that electrostatic interaction could dominate the binding between HH24 peptide and trastuzumab. Energy composition analysis further suggests that Ala32, His91, Tyr92, Thr93, and Thr94 in the light chain and Arg50, Trp99, Tyr105, Tyr33 in the heavy chain contribute most to the binding. It is worth noting that these residues belong to the CDR of trastuzumab (Fig. 1c and e). Moreover, the energy composition analysis of the HH24 peptide indicates that besides the recognition domain (QLGPYELWELSH), His6, Gly7, Gly9, and Ser10 also contribute to trastuzumab binding, which may impact the affinity between the mAb's recognition domain and HH24 (Fig. 1d). Overall, MST, docking and molecular dynamics simulation results showed that the HH24 peptide could have multiple interactions with the CDR in the Fab region, which can lead to moderate binding to trastuzumab.

3.2. Fabrication and characterization of the HH24 based affinity material

Inspired by the binding interactions between HER2 and trastuzumab (Fig. 2), the HH24 based biomimetic affinity material was fabricated in pipettes through a metal ion chelation reaction between Ni^{2+} based IMAC material and HH24 containing the histidine tag (Fig. S3). Moreover, to meet the high-throughput needs for clinical sample processing, multi-channel syringe pumps combined with this material in pipettes were used to simultaneously process a series of serum samples (Fig. 2). The resultant material was characterized by TGA, EDS, FT-IR, and SEM analyses. According to the TGA results, all material backbones were completely decomposed at 600 °C. A weight-loss difference of 1.043% was observed between the Ni^{2+} based IMAC material and poly(GMA-*co*-EDMA)-NTA, which indicated the successful immobilization of Ni^{2+} (Fig. 3a). EDS results revealed the existence of the Ni element in the

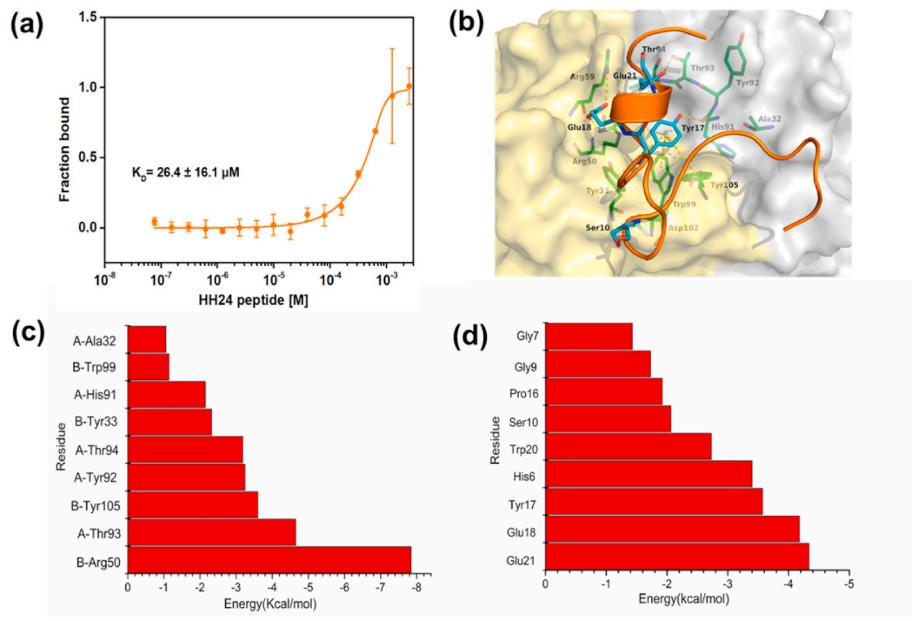

(e)

VL (variable region of light chain) with CDR 1, CDR 2, CDR 3:

DIQMTQSPSSLSASVGDRVTITC**RASQDVNTAVA**WYQQKPGKAPKLLI

↑32

Y**SASFLYS**GVPSRFSGSRSGTDFTLTISSLQPEDFATYYC**QQHYTTPPT**F

GQGTKVEIK

91-94

VH (variable region of heavy chain) with CDR 1, CDR 2, CDR 3:

EVQLVESGGGLVQPGGSLRLSCAAS**GFNIKDTYIH**WVRQAPGKGLEW

↑33

V**ARIYPTNGYTRYADSVKG**RFTISADTSKNTAYLQMNSLRAEDTAVYY

50 ↑↓99 ↓105

CSR**WGGDGFYAMDY**WGQGTLVTVSS

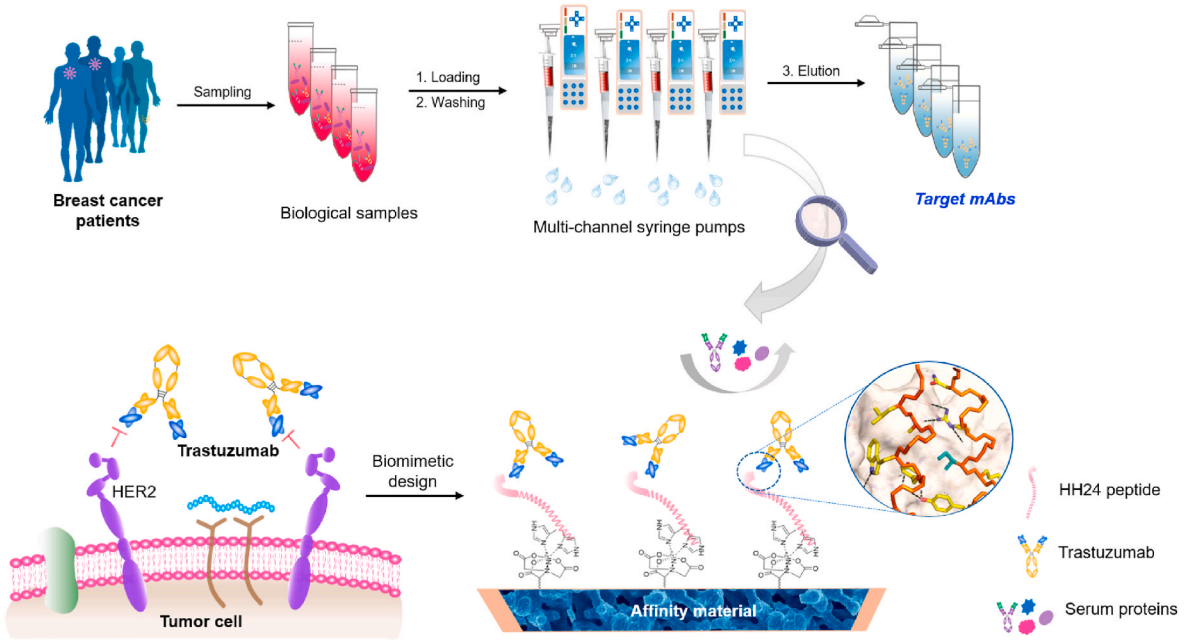

Fig. 1. MST and computational analysis results. **(a)** Binding curve for HH24 peptide with trastuzumab obtained by MST. Error bars represent standard deviations of three independent measurements. **(b)** Binding mode of HH24 peptide to trastuzumab. The interface of trastuzumab chain A (light chain) is shown as a grey surface, whereas the chain B (heavy chain) is shown as a yellow surface. HH24 peptide is shown as cyan cartoon, and key residues are depicted with sticks. **(c)** Energy decomposition of key residues of trastuzumab and **(d)** HH24 peptide. **(e)** CDR regions of trastuzumab in light and heavy chains. (For interpretation of the references to colour in this figure legend, the reader is referred to the Web version of this article.)

Fig. 2. Enrichment strategy based on the HH24 modified affinity material for the targeted purification of trastuzumab from biological fluids.

HH24 modified material, which further confirmed that Ni^{2+} was successfully attached to the polymeric matrix (Fig. 3b). The immobilization of HH24 was evidenced by FT-IR: the characteristic peak of the amide bonds of HH24 at 1637 cm^{-1} was observed in the FT-IR spectrum of the biomimetic material (Fig. 3c). The immobilized amount of HH24 was estimated by comparing the amount of HH24 loaded with that found in the effluent, and the results obtained by the BCA method indicated that 11 mg peptide ligand per mL of material were immobilized. SEM images show that the material possesses a porous structure and spherical units agglomerated into large clusters interdispersed by large-pore channels (Fig. 3d). The macropore size and porosity of the resulting material were measured to be 3.7 μm and 62.63%, respectively, using the mercury injection method (Fig. 3e). The hydrophilicity of the novel material was finally studied via water contact angle measurements. As depicted in Fig. 3f, water droplets spread very quickly on the surface of the material with a final contact angle of 21.9°. These observed features (high porosity and good hydrophilicity) of the novel material overcome the shortcomings of traditional support materials and were found beneficial for an efficient binding between the HH24 ligand on the material surface and the target protein.

3.3. *Specificity, dynamic binding capacity, and anti-fouling ability of affinity material*

To check the recognition ability of this material for the target mAb, various proteins including trastuzumab, HSA, lactoferrin, and thrombin (each protein concentration is 0.5 mg/mL), were chosen as test compounds. As shown in Fig. 4a, after enrichment, the SDS-PAGE analysis of each fraction indicated that no interference from other proteins was detected in the elution fractions. To further evaluate the specific recognition ability of the novel material for trastuzumab, the retention behavior of a protein mixture containing hIgG was also investigated (Fig. 4b). After treatment with the novel material, hIgG was only detected in the loading and washing fractions (Fig. 4b) while trastuzumab was only observed in the elution fractions (Fig. 4a), which indicated that the novel material could effectively discriminate between trastuzumab and hIgG. The excellent specificity was further verified by examining the retention of different proteins on a capillary column containing the material. As can be seen in Fig. 4c, only trastuzumab was specifically retained on the material, while the other four proteins (including hIgG) were fast eluted out of the column after injection. Therefore, the HH24 based affinity material exhibited good potential for targeted recognition of trastuzumab in complex samples containing hIgG, which is significantly superior to classical Protein A/G/L or fragment crystallizable (Fc)-specific peptide based affinity materials [32,41].

The dynamic binding capacity (DBC) of the novel material for trastuzumab was then determined (Details in Supporting information S1.4). The dynamic binding data were fitted to the Langmuir equation by the least-squares regression method (Fig. 4d). The maximum DBC and the dissociation constant K_d were calculated and found to be 16.4 mg/g of material and 2.6 μM, respectively. Interestingly, an affinity between

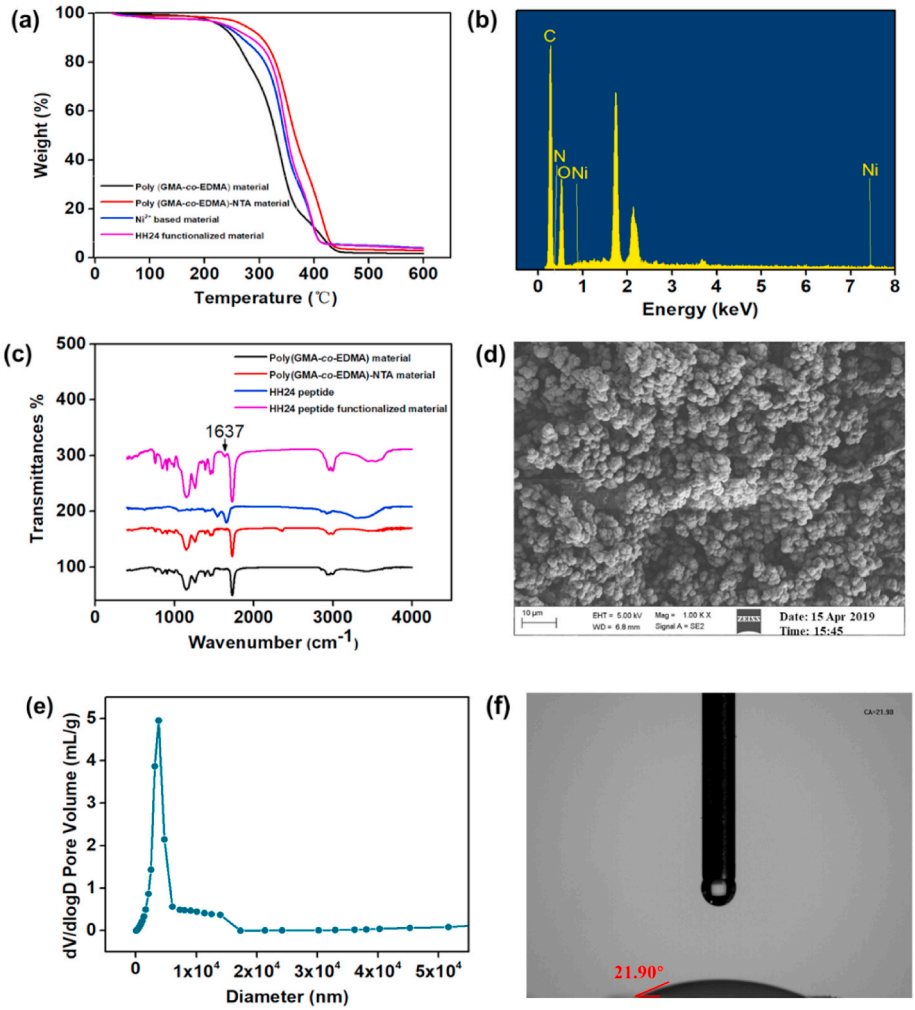

Fig. 3. TGA **(a)**, EDS **(b)**, FT-IR **(c)**, SEM **(d)**, pore size distribution **(e)** and water contact angle **(f)** analyses of the HH24 modified affinity material.

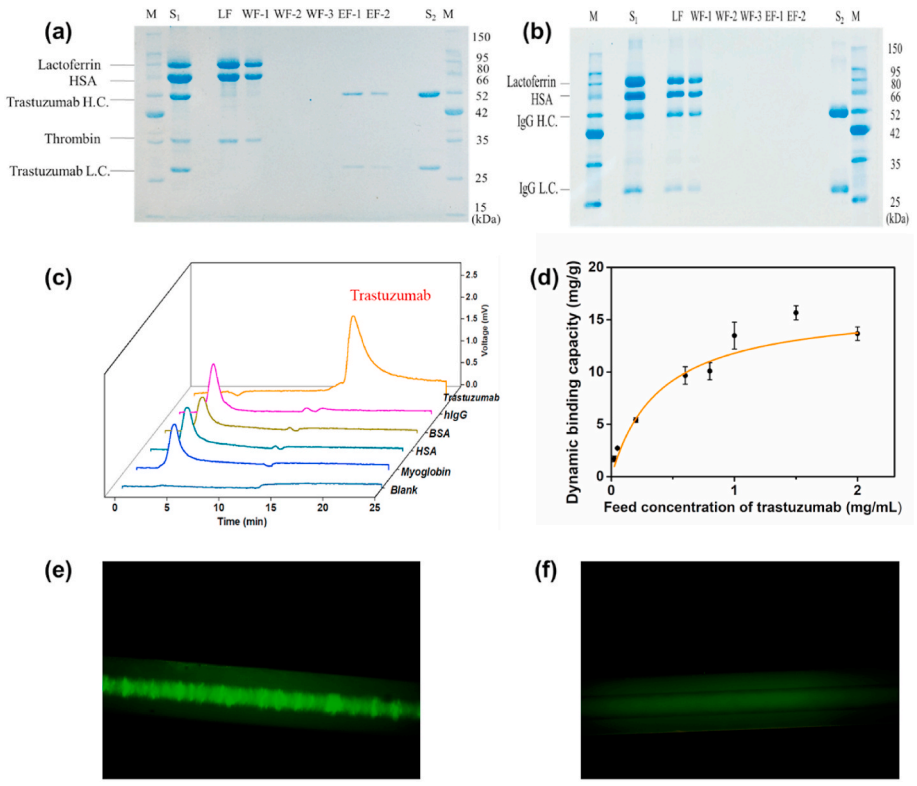

Fig. 4. Recognition ability of the HH24 peptide modified material for trastuzumab. **(a)** SDS-PAGE analysis (reducing conditions) of a protein mixture containing trastuzumab. Lanes: M, protein marker; S_1, standard protein mixture, S_2, standard trastuzumab; LF, loading fraction; WF, washing fractions; EF, elution fractions. **(b)** SDS-PAGE analysis (reducing conditions) of a protein mixture containing hIgG. **(c)** Retention of trastuzumab and other proteins on the novel material. Conditions: column dimensions: 150 mm × 100 μm I.D; mobile phase A, 20 mM PB, 150 mM NaCl, 0.05% Tween-20, pH 7.4; mobile phase B, 10 mM HCOONa, 100 mM NaCl, pH 3.1; switching point (mobile phase A to B): 10 min; UV detection wavelength: 280 nm; flow rate: 1 μL/min; injection volume: 1 μL. **(d)** Binding isotherm for trastuzumab on the HH24 peptide modified material. Fluorescence intensity of FITC-label BSA retained on the novel material **(e)** before washing and **(f)** after washing with buffer A.

HH24 peptide and trastuzumab in the low μM range makes elution milder. Moreover, the breakthrough curve of the new material was also determined at a flow rate of 1 mL/h and the binding capacity was obtained from the 10% point (Fig. S4). The binding capacity at 10% breakthrough was found to be 11.3 mg/mL, which is comparable to that previously reported for a Fc-specific peptide based polymer towards hIgG (9.0 mg/mL) [42]. The density (4.0 μmol/mL or 11 mg/mL) and affinity (K_d = 2.6 μM) of HH24 in the new material are lower than the peptide ligand density (12.3 μmol/mL or 25 mg/mL) and affinity (K_d = 345 nM) of the KH19 immobilized membrane towards trastuzumab. However, the binding capacity of the novel material is two times higher than that of the KH19 immobilized membrane (almost 5 mg/mL at 10% breakthrough) [35]. This may be attributed to the fact that a higher peptide density could cause a stronger steric shielding effect, so that the specific binding sites in the small peptide ligand may be less exposed to the target mAb.

Finally, the anti-nonspecific protein adsorption ability of the novel material was evaluated via FITC-labeled BSA fluorescence assay. As depicted in Fig. 4e and f, the fluorescence intensity of the FITC-labeled BSA in a capillary containing the material can be considered as almost negligible after flushing it with buffer A, which indicates that the material exhibits strong anti-fouling ability. Based on these results, it can be concluded that the HH24 modified material exhibits outstanding recognition ability for trastuzumab, suitable binding capacity, and good resistance to nontarget protein adsorption.

3.4. Highly specific capture and quantification of trastuzumab in serum samples

To evaluate the practical application potential of the novel material, human serum was diluted with buffer A and then spiked with trastuzumab (0.5 mg/mL final concentration). The influence of the pH of the elution buffer (10 mM HCOONa, 100 mM NaCl) on the purity and recovery of the enriched mAb was evaluated. As depicted in Fig. S5, after flushing with elution buffers at different pH values, only heavy (50 kDa) and light (25 kDa) chains of trastuzumab were observed on the SDS-PAGE image in the corresponding elution fractions. Moreover, the recovery of trastuzumab was enhanced with decreasing pH and then almost levelled off at pH 2.5–3.1 (90%).

Fig. 5a depicts representative SDS-PAGE results of spiked and blank 1:3 diluted serum samples under the optimal conditions. Good purity (98%) and recovery (90%) were achieved on the novel material with 20 mM PB, 150 mM NaCl, pH 7.4, 0.05% Tween-20 as the washing buffer (A) and 10 mM HCOONa, 100 mM NaCl, pH 3.1 as the elution buffer (B). The purity of the enriched protein was further verified by MALDI-TOF-MS (Fig. 5b and c). No protein was observed in the elution fraction of the blank serum, however two characteristic peaks were observed in the MS spectrum of the elution fraction of the spiked serum and assigned to trastuzumab (m/z: 148281 for z = 1 and m/z: 74564 for z = 2). These results indicate that the HH24 based affinity material possesses excellent specificity for trastuzumab and good antifouling ability towards serum proteins, allowing it to overcome the drawbacks of nonspecific adsorption observed with the previously reported Protein A/G/L [43] and KH19 based affinity materials [35]. In particular, the elution conditions are much milder than those used with the KH19 based affinity material (2% SDS, 100 mM DTT), so that they are not denaturating the target mAb (it was evidenced by the bioactivity evaluation of the enriched protein, showing in Supporting information S1.7 and Fig. S6). These advantages will be useful in the context of the investigation of trastuzumab biotransformation, but will also benefit to further study the impact of these biotransformation on antibody function (including antigen binding affinity, antibody-dependent cellular cytotoxicity, and complement-dependent cytotoxicity). Finally, the reusability of the resultant material was investigated. After 7 cycles of loading, washing, and elution, the material still showed relatively high specificity and recovery (Fig. 5d).

Based on the above results, the mAb was obtained with high purity from serum, and its quantification was easy achieved by fluorimetry. For these experiments, 1:3 diluted sera spiked with different concentrations of trastuzumab (0, 10, 30, 60, 80, 120 μg/mL) were firstly purified on

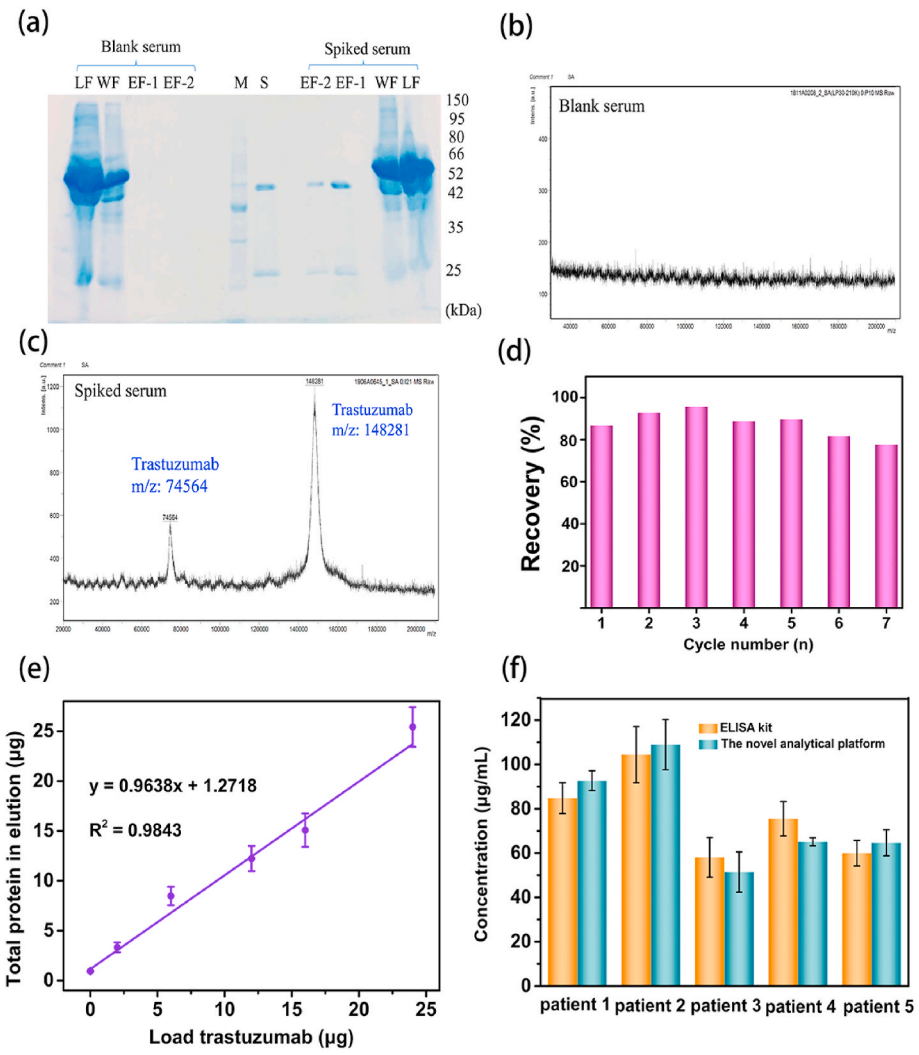

Fig. 5. Highly specific capture of trastuzumab from complex biological fluids. **(a)** Specificity of the novel material for trastuzumab in spiked human serum using SDS-PAGE analysis (reducing conditions). Lanes: LF, loading fraction; WF, washing fraction; EF, elution fractions; S, standard trastuzumab; M, protein marker. Left: blank serum, right: spiked serum. MALDI-TOF MS spectra of the elution fractions collected from **(b)** blank and **(c)** spiked human serum. **(d)** Reusability of the affinity material. (**e**) Correlation between the total protein content in eluted fractions purified on the HH24 based affinity material and trastuzumab standards using fluorescence spectrophotometry. Error bars represent standard deviations of experiments carried out with three replicate pipettes. (**f**) Comparison of results obtained with the fluorescence analysis and a commercial ELISA kit for the analysis of trastuzumab in breast cancer patient sera.

the HH24 based affinity material. The fluorescence intensity of the obtained eluates was measured and a standard curve was established by using solutions of trastuzumab standards in buffer B with concentrations ranging from 0 to 120 μg/mL. Fig. 5e showed that a good linear correlation was obtained between the total protein content in the eluates of spiked 1:3 diluted sera and the corresponding trastuzumab standards. Finally, the concentrations of trastuzumab in five patient sera were also tested and ranged from 50 to 110 μg/mL (Fig. 5f). These detected values were similar to those obtained with a commercial ELISA kit, which confirms the highly specific capture ability of the novel affinity material.

3.5. Evaluation of the reliability of the bioanalytical platform

For degradation study of trastuzumab, a specific platform was established by combining specific capture on the HH24 based affinity material, trypsin digestion, and LC-QTOF-MS using peptide mapping analysis. Some possible peptide modification sites are summarized in Table S2. To ensure the reliability of the platform, the influence of the enrichment process on the modification ratios of key peptide sequences was first investigated. As can be seen in Fig. S7, no obvious serum protein interference was observed by comparing blank and trastuzumab-spiked serum samples (all samples were analyzed after treatment with the affinity material), which further verifies the excellent specificity of the HH24 based affinity material. Moreover, we compared the modification ratios of key peptide sequences of trastuzumab obtained via direct digestion and after sample pretreatment (trastuzumab-spiked phosphate buffer was enriched using the HH24 based material and then digested). As shown in Fig. S8, no significant changes in modification ratios (such as deamidation, isomerization, oxidation, and glutamic acid cyclization) were found in these spiked PB samples, which indicates that the total pretreatment process has not induced significant artifacts. Therefore, the platform could exhibit good application potential for the in vitro/in vivo degradation analysis of trastuzumab in biological fluids.

3.6. In vitro degradation analysis of trastuzumab in time-course studies

To further evaluate the platform's capabilities, the analysis of the modification sites and rates was performed in PB and serum samples spiked with trastuzumab over an extended period of time (0, 4, 7, 14, 21 days). As depicted in Fig. 6, after incubation in PB for 21 days, the acidic charge variants were increased with a corresponding decrease in the main peak, but almost no change in the basic charge variants was observed. Some modifications could lead to antibody charge variants, such as asparagine deamidation, aspartic acid isomerization, methionine oxidation, and N-terminal glutamic acid cyclization [44]. To study the possible effect of trastuzumab modifications on the binding to the affinity material, the degradation analysis of all incubated PB samples was performed after enrichment on the affinity material. For comparison, these incubated samples were also directly digested and analyzed by LC-QTOF-MS. As shown in Fig. 7, the level of deamidation of LC-Asn-30 to aspartic acid (located in the CDR1 of the light chain) was found to be greatly increased from 9% to 62% (direct digestion) and

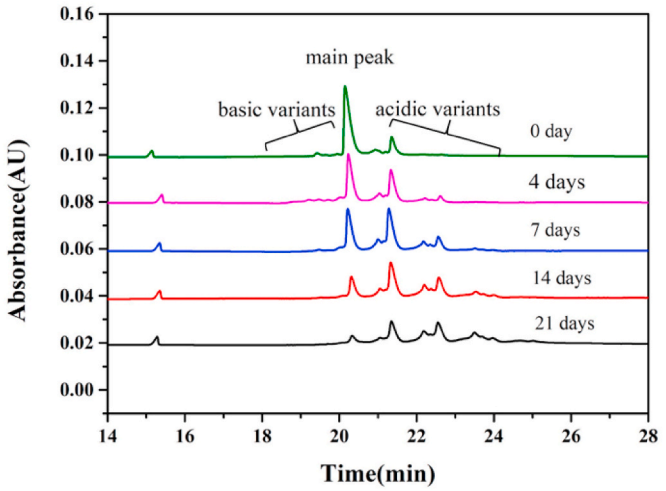

Fig. 6. CZE analysis of trastuzumab in spiked PB samples after incubation at 37 °C.

61% (after enrichment) over the studied period, whereas the extent of deamidation of HC-Asn-55 and isomerization to isoaspartic acid (located in the CDR2 of the heavy chain) was only moderately affected, such as from 7.43% to 17.18% (direct digestion) and 20.48% (after enrichment) for isomerization. However, the conversion of Asn55 to aspartic acid (Asp55) and the concomitant isomerization to isoaspartic acid (iso-Asp55) could lead to a significant decrease (>70%) of bioactivity due to a reduction in receptor binding affinity [17,45]. Moreover, the deamidation of HC-Asn-387/392/393 in the constant C_H3 region of the heavy chain was also observed and dramatically increased over time. In addition, the oxidation of methionine residues was found in some key peptide sequences, such as LC-Met-4, HC-Met-83, HC-Met-107 (located in the variable region of the light or heavy chain), HC-Met-255, and HC-Met-431 (located in the constant region of the heavy chain), which could impact the binding to the antigen or the neonatal Fc receptor (FcRn) [11]. Slight changes in glutamic acid (HC-E-1) cyclization (located in the variable region, near the CDR of the target mAb) were also observed with increasing incubation time [12]. It is worth noting that the in vitro degradation trends and sites in the target mAb observed after pretreatment on the affinity material were consistent with those obtained by direct digestion, which verifies the reliability of the proposed platform for peptide modification analysis.

Compared to PB, more physiologically relevant in vitro studies can

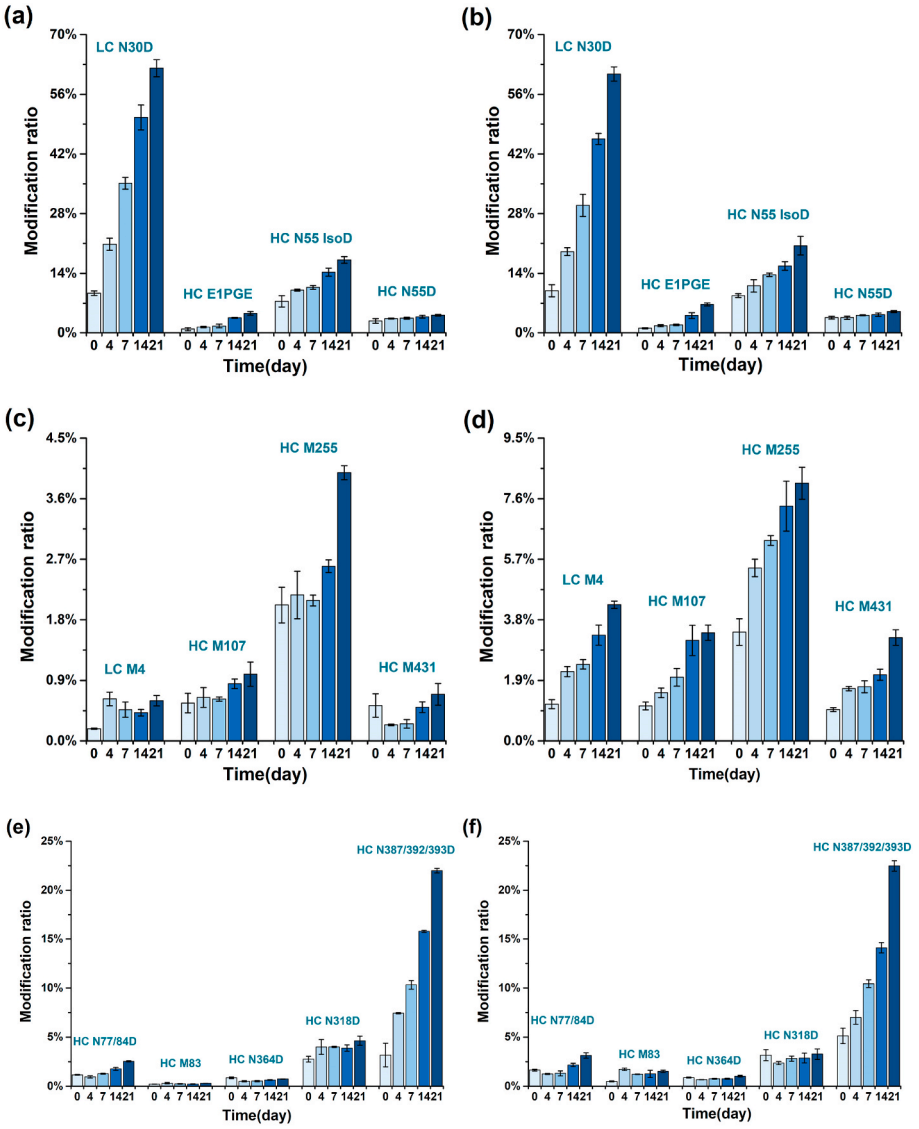

Fig. 7. Degradation analysis of trastuzumab in spiked PB samples after incubation at 37 °C (direct digestion: a, c, e; after pretreatment: b, d, f).

be conducted in biological fluids like serum since they provide a rich source of proteins and metabolites [13]. Therefore, the degradation of trastuzumab at different concentrations (0.2 mg/mL and 0.5 mg/mL) in spiked human serum was also investigated using this platform. As shown in Fig. S9, the degradation rates for the target mAb were slightly increased at higher drug concentration. Moreover, due to a catalytic effect of plasma proteins, the deamidation rate of proteins in plasma was faster than in PB buffer at same pH7.4 [46]. Therefore, deamidation of LC-Asn-30 and HC-Asn-387/392/393 during serum incubation (Figs. S9b and S9f) occurs at least 1.5-fold faster than that of in PB buffer (Fig. 7b and f). The degradation trends for other studied peptides in serum were similar to those observed in PB at the same drug concentration (0.5 mg/mL). These results further demonstrate that the platform has a good potential for studying the degradation of the target mAb in complex biological fluids. In the early stages of drug development, in vitro study with spiked serum sample could be used to support risk assessment by understanding and predicting in vivo results.

3.7. Biotransformation analysis of trastuzumab in patient serum samples

Although several major degradation pathways could be examined using in vitro models, peptide modifications for the target mAb may still have different dynamics in vivo because of differences in multiple factors, such as the Ig subclass, mechanism of action, affinity to target, nonspecific affinity, drug delivery system, antibody engineering, as well as the clinical indication, dosage and administration regimen, and individual variations [13,47]. Therefore, the applicability of the proposed platform was further investigated by studying the in vivo biotransformation of trastuzumab in a series of HER2-positive breast cancer patient serum samples. Compared to the spiked PB samples (Fig. 7), moderate Asn deamidation or Asp isomerization, were observed on the key CDR sites (LC-Asn-30, HC-Asn-55), variable region sites (HC-Asn-77/84), and constant region sites (HC-Asn-318, HC-Asn-364, HC-Asn-387/392/393) of the antibody (Fig. 8). Moreover, the oxidation levels of HC-Met-107/255/431 for the target mAb in some patient sera were slightly higher than those observed in the spiked PB and serum samples incubated in vitro. Differences in modification degrees were also observed between patients. Compared to previously reported methods for in vivo analysis, the novel platform based on trastuzumab capture on the HH24 modified affinity material exhibited superior specificity for the target mAb than classical Protein A/G/L based analytical methods [43,48], lower cost and higher stability than antigen or anti-idiotypic antibody based analytical methods [13,49], and enabled comprehensive evaluation of modification sites. Thus, the novel platform has a great application potential for studying the biotransformation of the target mAb in patients.

4. Conclusions

In this study, a novel bioanalytical platform was successfully constructed by combining specific capture on HER2 mimotope peptide HH24 based affinity material, trypsin digestion, and LC-QTOF-MS for in vitro/in vivo degradation analysis of trastuzumab. Due to the high specificity of the HH24 ligand to the CDR of trastuzumab and good antifouling ability of the polymeric matrix, the novel material exhibited outstanding enrichment performances for trastuzumab in serum samples and thus overcame the shortcomings of traditional Protein A/G/L, antigen, and mimotope peptide based materials. Based on its superior enrichment performance, some key modification sites, which could affect the binding activity of the target mAb to the antigen or FcRn, were detected and their modification degrees were determined by this platform. Moreover, similar modification sites were also found by studying

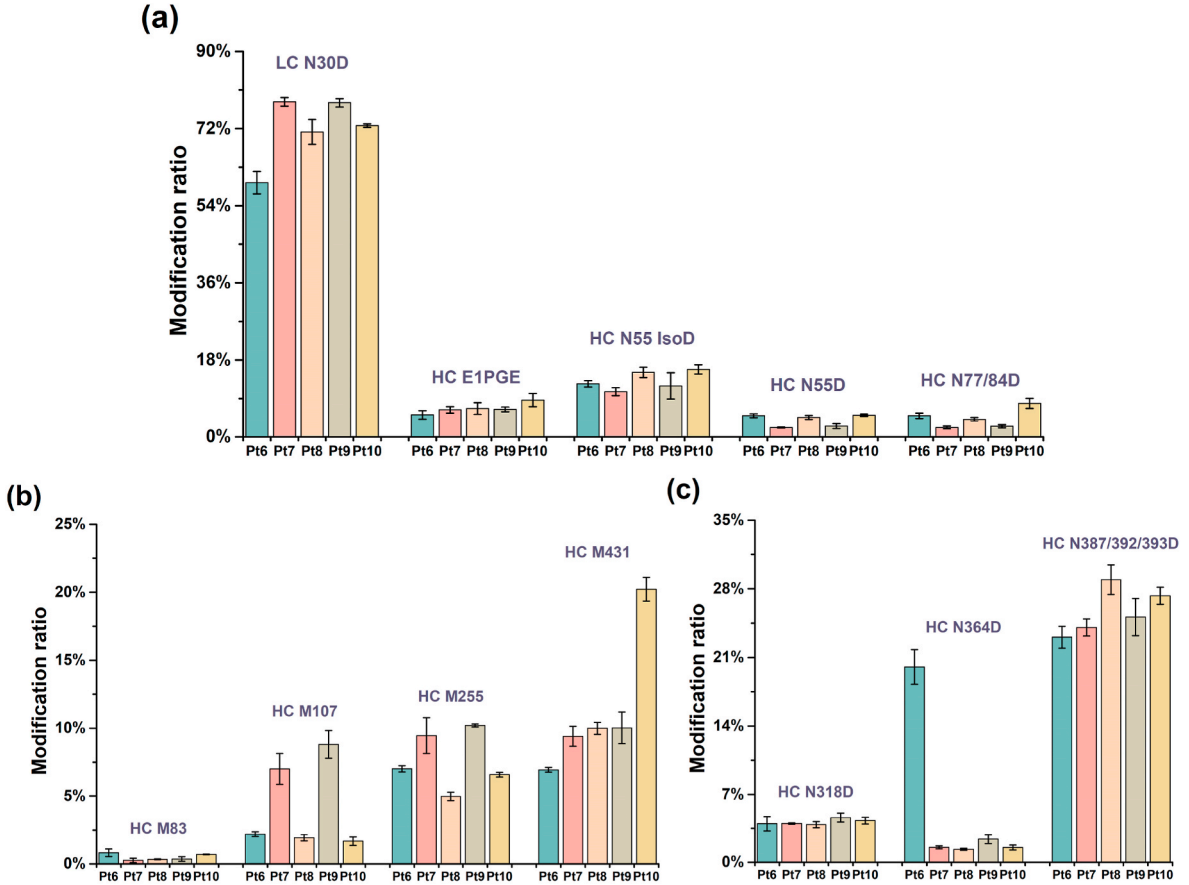

Fig. 8. Biotransformation analysis of trastuzumab in patient serum samples.

the biotransformation of trastuzumab in a series of HER2-positive breast cancer patient serum samples. These key amino acids that get modified rapidly may need to be controlled more tightly during the manufacturing process to preserve product efficacy. In the near future, the application potential of this bioanalytical platform will be further investigated by studying the degradation or biotransformation of trastuzumab-related products.

CRediT authorship contribution statement

Li Lu: carried out the experiments, analyzed data and wrote the paper. **Xiao Liu:** carried out the experiments, analyzed data and wrote the paper. **Chengyi Zuo:** carried out some experiments and analyzed the related data. **Jingwei Zhou:** carried out some experiments and analyzed the related data. **Chendi Zhu:** carried out some experiments and analyzed the related data. **Zhang Zhang:** carried out some experiments and analyzed the related data. **Marianne Fillet:** edited the article. **Jacques Crommen:** edited the article. **Zhengjin Jiang:** designed the project and provided overall guidance. **Qiqin Wang:** designed the project and provided overall guidance. All authors reviewed the manuscript.

Declaration of competing interest

The authors declare that they have no known competing financial interests or personal relationships that could have appeared to influence the work reported in this paper.

Data availability

The data that has been used is confidential.

Acknowledgements

This work was supported by the National Natural Science Foundation of China (Grant: 82173773, 82073806), the Natural Science Foundation of Guangdong Province, China (Grant: 2021A0505030039, 2022A1515011576), and Science and Technology Program of Guangzhou, China (Grant: 202102020729).

Appendix A. Supplementary data

Supplementary data to this article can be found online at https://doi.org/10.1016/j.aca.2022.340199.

References

[1] G.J. Weiner, Building better monoclonal antibody-based therapeutics, Nat. Rev. Cancer 15 (2015) 361–370.
[2] A.M. Scott, J.D. Wolchok, L.J. Old, Antibody therapy of cancer, Nat. Rev. Cancer 12 (2012) 278–287.
[3] H. Kaplon, A. Chenoweth, S. Crescioli, J.M. Reichert, Antibodies to watch in 2022, mAbs 14 (2022), e2014296.
[4] G. Walsh, Biopharmaceutical benchmarks 2018, Nat. Biotechnol. 36 (2018) 1136–1145.
[5] J.F. Kellie, M.Z. Karlinsey, Review of approaches and examples for monitoring biotransformation in protein and peptide therapeutics by MS, Bioanalysis 10 (2018) 1877–1890.
[6] S. Schadt, S. Hauri, F. Lopes, M.R. Edelmann, R.F. Staack, R. Villaseñor, H. Kettenberger, A.B. Roth, F. Schuler, W.F. Richter, C. Funk, Are biotransformation studies of therapeutic proteins needed? Scientific considerations and technical challenges, Drug Metab. Dispos. 47 (2019) 1443–1456.
[7] C. Nowak, A. Tiwari, H.C. Liu, Asparagine deamidation in a complementarity determining region of a recombinant monoclonal antibody in complex with antigen, Anal. Chem. 90 (2018) 6998–7003.
[8] Y. Wang, X. Li, Y. Liu, D. Richardson, H. Li, M. Shameem, X. Yang, Simultaneous monitoring of oxidation, deamidation, isomerization, and glycosylation of monoclonal antibodies by liquid chromatography-mass spectrometry method with ultrafast tryptic digestion, mAbs 8 (2016) 1477–1486.
[9] O. Olaleye, B. Spanov, R. Ford, N. Govorukhina, N.C. van de Merbel, R. Bischoff, Enrichment and liquid chromatography-mass spectrometry analysis of trastuzumab and pertuzumab using affimer reagents, Anal. Chem. 93 (2021) 13597–13605.
[10] Y. Yan, H. Wei, Y. Fu, S. Jusuf, M. Zeng, R. Ludwig, S.R. Krystek Jr., G.D. Chen, L. Tao, T.K. Das, Isomerization and oxidation in the complementarity-determining regions of a monoclonal antibody: a study of the modification-structure-function correlations by hydrogen-deuterium exchange mass spectrometry, Anal. Chem. 88 (2016) 2041–2050.
[11] J. Mo, Q. Yan, C. Kwong So, T. Soden, M.J. Lewis, P. Hu, Understanding the impact of methionine oxidation on the biological functions of IgG1 antibodies using hydrogen/deuterium exchange mass spectrometry, Anal. Chem. 88 (2016) 9495–9502.
[12] L.M. Bersin, S.M. Patel, E.M. Topp, Effect of 'pH' on the rate of pyroglutamate formation in solution and lyophilized solids, Mol. Pharm. 18 (2021) 3116–3124.
[13] N. Yang, Q. Tang, P. Hu, M.J. Lewis, Use of in vitro systems to model in vivo degradation of therapeutic monoclonal antibodies, Anal. Chem. 90 (2018) 7896–7902.
[14] S. Kaur, K.P. Bateman, J. Glick, M. Jairaj, J.F. Kellie, J. Sydor, J.N. Zeng, IQ consortium perspective: complementary LBA and LC-MS in protein therapeutics bioanalysis and biotransformation assessment, Bioanalysis 12 (2020) 257–270.
[15] Y. Li, M. Monine, Y. Huang, P. Swann, I. Nestorov, Y. Lyubarskaya, Quantitation and pharmacokinetic modeling of therapeutic antibody quality attributes in human studies, mAbs 8 (2016) 1079–1087.
[16] Y. Zhang, S. Wu, Y. Li, Comparative study of profiling post-translational modifications of a circulating antibody drug in human with different capture reagents, Biologicals 45 (2017) 93–95.
[17] P. Bults, R. Bischoff, H. Bakker, J.A. Gietema, N.C. van de Merbel, LC-MS/MS-Based monitoring of in vivo protein biotransformation: quantitative determination of trastuzumab and its deamidation products in human plasma, Anal. Chem. 88 (2016) 1871–1877.
[18] B.V. Ayyar, S. Arora, C. Murphy, R. O'Kennedy, Affinity chromatography as a tool for antibody purification, Methods 56 (2012) 116–129.
[19] S.H. Lee, Y. Hoshino, A. Randall, Z. Zeng, P. Baldi, R.A. Doong, K.J. Shea, Engineered synthetic polymer nanoparticles as IgG affinity ligands, J. Am. Chem. Soc. 134 (2012) 15765–15772.
[20] Y. Liu, Y. Lu, Z. Liu, Restricted access boronate affinity porous monolith as a protein A mimetic for the specific capture of immunoglobulin G, Chem. Sci. 3 (2012) 1467–1471.
[21] T. Barroso, A. Hussain, A.C.A. Roque, A. Aguiar-Ricardo, Functional monolithic platforms: chromatographic tools for antibody purification, Biotechnol. J. 8 (2013) 671–681.
[22] Q. Wang, H. Jin, D. Xia, H. Shao, K. Peng, X. Liu, H. Huang, Q. Zhang, J. Guo, Y. Wang, J. Crommen, N. Gan, Z. Jiang, Biomimetic polymer-based method for selective capture of C-reactive protein in biological fluids, ACS Appl. Mater. Interfaces 10 (2018) 41999–42008.
[23] H. Yang, P.V. Gurgel, R.G. Carbonell, Purification of human immunoglobulin G via Fc-specific small peptide ligand affinity chromatography, J. Chromatogr. A 1216 (2009) 910–918.
[24] W.W. Zhao, Q.H. Shi, Y. Sun, Dual-ligand affinity systems with octapeptide ligands for affinity chromatography of hIgG and monoclonal antibody, J. Chromatogr. A 1369 (2014) 64–72.
[25] A. Xue, W.W. Zhao, X. Liu, Y. Sun, Affinity chromatography of human IgG with octapeptide ligands identified from eleven peptide-ligand candidates, Biochem. Eng. J. 107 (2016) 18–25.
[26] S. Menegatti, A.D. Naik, R.G. Carbonell, The hidden potential of small synthetic molecules and peptides as affinity ligands for bioseparations, Pharm. Bioproc. 1 (2013) 467–485.
[27] L. Yang, L. Zhang, L. Yan, H. Zheng, P. Lu, J. Chen, J. Dai, H. Sun, Y. Xu, T. Yang, Stability assessment of a new antithrombotic small peptide, Arg-Gly-Asp-Trp-Arg (RGDWR), and its derivative, Biotechnol. Lett. 39 (2017) 1183–1190.
[28] Y.M. Fang, D.Q. Lin, S.J. Yao, Review on biomimetic affinity chromatography with short peptide ligands and its application to protein purification, J. Chromatogr. A 1571 (2018) 1–15.
[29] Y. He, S. Xie, X. Yang, R. Yuan, Y. Chai, Electrochemical peptide biosensor based on in situ silver deposition for detection of prostate specific antigen, ACS Appl. Mater. Interfaces 7 (2015) 13360–13366.
[30] J. Navarro-Sanchez, A.I. Argente-Garcia, Y. Moliner-Martinez, D. Roca-Sanjuan, D. Antypov, P. Campins-Falco, M.J. Rosseinsky, C. Marti-Gastaldo, Peptide metal-organic frameworks for enantioselective separation of chiral drugs, J. Am. Chem. Soc. 139 (2017) 4294–4297.
[31] K. Du, Peptide immobilized monolith containing tentacle-type functionalized polymer chains for high-capacity binding of immunoglobulin G, J. Chromatogr. A 1374 (2014) 164–170.
[32] X. Wang, D. Xia, H. Han, K. Peng, P. Zhu, J. Crommen, Q. Wang, Z. Jiang, Biomimetic small peptide functionalized affinity monoliths for monoclonal antibody purification, Anal. Chim. Acta 1017 (2018) 57–65.
[33] B. Jiang, W. Liu, H. Qu, L. Meng, S. Song, T. Ouyang, C. Shou, A novel peptide isolated from a phage display peptide library with trastuzumab can mimic antigen epitope of HER-2, J. Biol. Chem. 280 (2005) 4656–4662.
[34] E. Favoino, M. Prete, G. Catacchio, G. Conteduca, F. Perosa, CD20-Mimotope peptides: a model to define the molecular basis of epitope spreading, Int. J. Mol. Sci. 20 (2019) 1920.
[35] W. Liu, A.L. Bennett, W. Ning, H. Tan, J.D. Berwanger, X. Zeng, M.L. Bruening, Monoclonal antibody capture and analysis using porous membranes containing immobilized peptide mimotopes, Anal. Chem. 90 (2018) 12161–12167.
[36] J.D. Berwanger, H.Y. Tan, G. Jokhadze, M.L. Bruening, Determination of the serum concentrations of the monoclonal antibodies bevacizumab, rituximab, and panitumumab using porous membranes containing immobilized peptide mimotopes, Anal. Chem. 93 (2021) 7562–7570.

[37] C.J. Chen, M.C. Tseng, H.J. Lin, T.W. Lin, Y.R. Chen, Visual indicator for surfactant abundance in MS-based membrane and general proteomics applications, Anal. Chem. 82 (2010) 8283–8290.
[38] O. Spiga, A. Bernini, M. Scarselli, L. Giovannoni, F. Laschi, P. Neri, L. Bracci, L. Lozzi, N. Niccolai, Histidyl tags and structural stabilization of linear peptides, Spectrosc. Lett. 35 (2002) 111–118.
[39] K.A. Majorek, M.L. Kuhn, M. Chruszcz, W.F. Anderson, W. Minor, Double trouble-Buffer selection and His-tag presence may be responsible for nonreproducibility of biomedical experiments, Protein Sci. 23 (2014) 1359–1368.
[40] Q. Wang, K. Peng, N. Gan, X. Liu, H. Huang, H. Shao, H. Jin, J. Crommen, Z. Jiang, Rapid fabrication of versatile zwitterionic super-hydrophilic polymers by sole-monomer system for biomolecules separation, Chem. Eng. J. 396 (2020), 125121.
[41] Q. Luo, H. Zou, Q. Zhang, X. Xiao, J. Ni, High-performance affinity chromatography with immobilization of protein A and L-histidine on molded monolith, Biotechnol. Bioeng. 80 (2002) 481–489.
[42] F. Tehrani Najafian, N.S. Bibi, T. Islam, M. Fernandez-Lahore, A megaporous material harbouring a peptide ligand for affinity IgG purification, Electrophoresis 38 (2017) 2914–2921.
[43] E.N. Fung, P. Bryan, A. Kozhich, Techniques for quantitative LC-MS/MS analysis of protein therapeutics: advances in enzyme digestion and immunocapture, Bioanalysis 8 (2016) 847–856.
[44] D.R. Stoll, D.C. Harmes, J. Danforth, E. Wagner, D. Guillarme, S. Fekete, A. Beck, Direct identification of rituximab main isoforms and subunit analysis by online selective comprehensive two-dimensional liquid chromatography-mass spectrometry, Anal. Chem. 87 (2015) 8307–8315.
[45] D. Chelius, D.S. Rehder, P.V. Bondarenko, Identification and characterization of deamidation sites in the conserved regions of human immunoglobulin gamma antibodies, Anal. Chem. 77 (2005) 6004–6011.
[46] S. Yin, C.V. Pastuskovas, L.A. Khawli, J.T. Stults, Characterization of therapeutic monoclonal antibodies reveals differences between in vitro and in vivo time-course studies, Pharm. Res. (N. Y.) 30 (2013) 167–178.
[47] Y. Li, Y. Huang, J. Ferrant, Y. Lyubarskaya, Y. Zhang, S. Li, S. Wu, Assessing in vivo dynamics of multiple quality attributes from a therapeutic IgG4 monoclonal antibody circulating in cynomolgus monkey, mAbs 8 (2016) 961–968.
[48] T.G. Halvorsen, L. Reubsaet, Antibody based affinity capture LC-MS/MS in quantitative determination of proteins in biological matrices, TRAC Trend. Anal. Chem. 95 (2017) 132–139.
[49] L. Huang, J. Lu, V.J. Wroblewski, J.M. Beals, R.M. Riggin, In vivo deamidation characterization of monoclonal antibody by LC/MS/MS, Anal. Chem. 77 (2005) 1432–1439.